High-Performance Evanescently Edge Coupled Photodiodes With Partially p-Doped Photoabsorption Layer at 1.55-μm Wavelength

Y.-S. Wu, J.-W. Shi, J.-Y. Wu, F.-H. Huang, Y.-J. Chan, Y.-L. Huang, and R. Xuan

***Abstract*—In this letter, we demonstrate a high-performance evanescently coupled photodiode (ECPD) with the partially p-doped photoabsorption layer. As compared to the control ECPD with the traditional intrinsic photoabsorption layer, the demonstrated device can exhibit much higher output saturation current (power) and electrical bandwidth without sacrificing the quantum efficiency performance. By properly designing the geometry size and epilayer structures of the partially p-doped ECPD, very high responsivity (1.01 A/W), high electrical bandwidth (around 50 GHz), and high saturation current bandwidth product (920 mA · GHz, at 40 GHz) have been achieved simultaneously at 1.55-μm wavelength.**

***Index Terms*—Evanescent coupling, high efficiency, high-power photodiode, optical receivers, photodiode.**

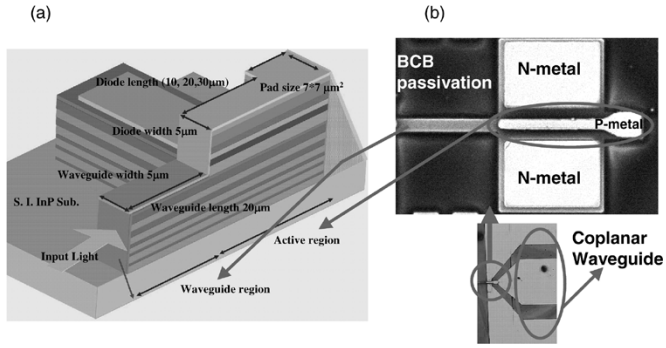

Fig. 1. (a) Cross-sectional view and (b) top view of demonstrated ECPDs.

THERE ARE two major trends to meet the challenge of photodetectors (PDs) with wide electrical bandwidth, high responsivity, and high output saturation power performance [1]. One is to distribute and uniform the photocurrents along the edge-coupled PDs, such as, velocity matched distributed photodetector [2] and evanescent coupled photodiode (ECPD) [3]–[5]; the other is to minimize the space-charge effect in the photoabsorption volume by changing the structure or material of epitaxial layers, such as unitraveling carrier PD [6], partially depleted absorber photodiode [7], and low-temperature-grown GaAs-based PDs [8]. However, the quantum efficiency performance of PDs with high saturation power are usually sacrificed due to its thin intrinsic layer or the recombination process of photogenerated carriers in the photoabsorption layer with p-type dopant or high density of defect [1], [8]. Recently, Muramoto and Ishibashi have demonstrated a new photodiode design that combines the depleted and neutral absorption layers (p-type doping) to maximize the bandwidth-efficiency product of photodiode [9]. In this work, we incorporated the partially p-doped photoabsorption layer and the evanescently edge-coupled waveguide structure of photodiode [10] to maximize its electrical bandwidth, quantum efficiency, and the capability of radio-frequency (RF) power generation. As compared to the control ECPD with the traditional intrinsic photoabsorption layer, the demonstrated ECPD with p-doped photoabsorption layer can achieve superior high-power performance without sacrificing the quantum efficiency. Very high responsivity (1.01 A/W), high electrical bandwidth (around 50 GHz), and high saturation current bandwidth product performances (more than 920 mA · GHz at 40 GHz) have been achieved simultaneously at 1.55-μm wavelength regime.

In order to study the influence of partially p-doped photoabsorption layers on the high-power performance of photodiode, two kinds of devices, which have the same structures of epilayers except for the photoabsorption active region, were fabricated. Device A has the graded partially p-doped photoabsorption layer to accelerate the drift velocity of photogenerated electrons [6], [12]and Device B has a pure intrinsic photoabsorption layer. The cross-sectional schematic diagram and top view of both devices are given in Fig. 1(a) and (b), respectively. As shown in Fig. 1(a), we adopted a short (20 μm) multimode waveguide that consists of a diluted waveguide and two optical matching layers [10]. The diluted waveguide is composed of five InGaAsP layers with 20-, 50-, 80-, 110-, and 140-nm thickness, interspersed between the 400-nm-thick InP layers. The number of periods has been optimized to achieve high coupling efficiency with an input fiber [10], [11]. The two optical matching layers are n^+-doped InGaAsP (1×10^{18} cm^{-3}) for good n-type ohmic contacts and acceptable free carrier loss [10]. The optical design and simulation of our demonstrated structure were achieved by using the commercialized three-dimensional beam propagation method software, and the detail thickness and composition of each epilayer are given in [12].

The epitaxial layer structures of the demonstrated devices were grown by metal–organic chemical vapor deposition on a

Manuscript received October 15, 2004; revised December 6, 2004. This work was supported by the National Science Council of Taiwan under Grant NSC 92-2218-E-008-011 and Grant 93-2215-E-008-022.

Y.-S. Wu, J.-W. Shi, J.-Y. Wu, F.-H. Huang, and Y.-J. Chan are with the Department of Electrical Engineering, National Central University, Taoyuan 320, Taiwan, R.O.C. (e-mail: jwshi@ee.ncu.edu.tw).

Y.-L. Huang and R. Xuan are with the Optoelectronic Modules and Packaging Department, Optical Communication and Optoelectronic Components, Industrial Technology Research Institute, Hsinchu 320, Taiwan, R.O.C.

Digital Object Identifier 10.1109/LPT.2005.844010

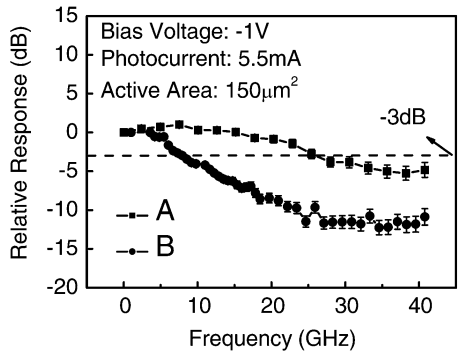

Fig. 2. Measured frequency responses of Devices A and B under the same high output current (5.5 mA) and dc bias voltage (-1 V). The active area of Devices A and B is about 150 μm^2.

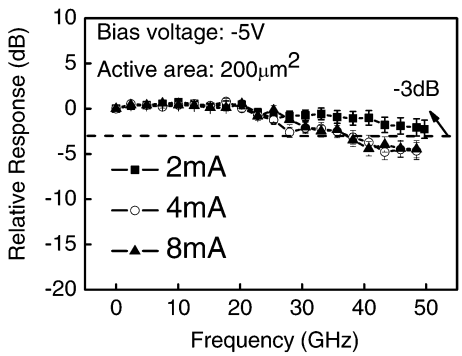

Fig. 3. Measured frequency responses of Device A under three different output photocurrent (closed square: 2 mA; open circle: 4 mA; and closed triangle: 8 mA). The dc bias voltage is fixed at -5 V and the active area of device is 200 μm^2. The $f_{3\ \mathrm{dB}}$ is around 50 GHz under 2-mA photocurrent operation.

semi-insulating (SI) substrate.[1] Both devices were fabricated by use of the standard photolithography, metallization, liftoff, and dry etching processes. The active area of photodiode was defined by the p-type metallization and dry etching process. In the polarization process, we adopted the bisbenzocyclobutene (BCB) film, which can not only significantly reduce the dark current of photodiode but also reduce its parasitic capacitance. As shown in Fig. 1(b), a coplanar waveguide, which is connected with the active area of photodiodes, was fabricated on the SI InP substrate for high-speed measurement. Finally, the devices were precisely cleaved ($\pm$5-μm accuracy) by patterning a V-groove, which was formed by the wet-etching process, and an antireflection coating was deposited on the facet.

We employed a tunable semiconductor laser as the light source which has a 1550-nm center wavelength for the dc photocurrent measurement. The measured Devices A and B have similar geometry sizes and exhibit almost the same values of responsivity [12]. When the absorption length of Device A is over 20 μm (active area is larger than 150 μm^2), a very high responsivity (1.01 A/W) [10] can be achieved [12]. These results indicate that the partially p-doped photoabsorption layer of our structure will not degrade the performance of quantum efficiency. As compared to the reported responsivity of the ECPDs with an integrated taper, the responsivity of our structure is significantly higher due to much shorter coupling length (20 versus 700 μm) and lower optical scattering loss of device [3]–[5].

The bandwidth and saturation current were measured with a heterodyne beating setup [3], [10], [13].

The measured frequency responses and $f_{3\mathrm{dB}}$ electrical bandwidths of Devices A and B are shown in Fig. 2. Devices A and B have the same size of active area (150 μm^2) under the same dc bias voltage (-1 V) and output photocurrent (5.5 mA). The influences of microwave probe, RF cable, RF bias tee, and RF adapters on the measured frequency responses were removed by use of the RF correction technique and a 50-GHz network analyzer [14]. We have added error-bars in all the measured frequency responses (Figs. 2 and 3) of both devices to represent the fluctuations of measured RF power during experiment. The values of added error bars depend on the degree of fluctuation

[1]The epilayers are supported by Land Mark Optoelectronics Corp., Tainan, Taiwan, R.O.C.

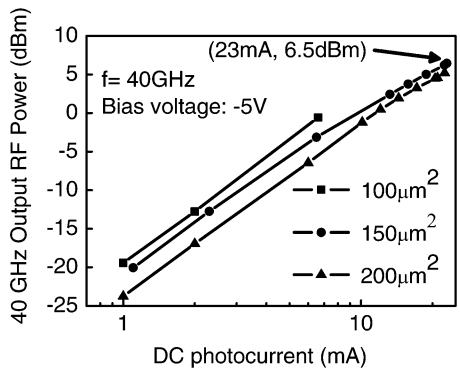

Fig. 4. RF power versus dc photocurrent of Device A with three different active areas (closed square: 100 μm^2; closed circle: 150 μm^2; closed triangle: 200 μm^2) at 40-GHz operating frequency and a fixed dc bias voltage (-5 V). The operation condition for maximum output current and power are shown in the figure.

of obtained RF signal, which fluctuates more seriously under low photocurrent (2 mA), low bias voltage (-1 V), or high frequency (>40 GHz) operation. According to the measurement results, we can clearly see that Device A with partially p-doped photoabsorption layer has superior electrical bandwidth performance ($\sim$26 versus $\sim$8 GHz) especially under high current (5.5 mA) and low bias voltage operation (-1 V). In order to further study the speed and power performances of Device A, we have measured its frequency responses under different conditions of large signal operation. Fig. 3 shows the measured frequency responses of Device A with 200 μm^2 active area under the same dc bias (-5 V) and different output photocurrent (2, 4, and 8 mA). Each trace (2, 4, and 8 mA) is normalized to its own value of RF power at near dc frequency. The $f_{3\mathrm{dB}}$ electrical bandwidth is around 50 GHz under 2-mA output photocurrent, and it only slightly degrades to around 40 GHz when the output photocurrent increases to 8 mA. The obtained high responsivity (1.01 A/W) and high electrical bandwidth under high current operation (around 40 GHz at 8 mA) of demonstrated device ensure its applications to 40-Gb/s analog and digital fiber communication system.

Three traces in Fig. 4 represent the photogenerated RF power versus dc photocurrent of Device A with three different active areas (100, 150, 200 μm^2). The operating frequency and dc bias voltage is fixed at 40 GHz and -5 V, respectively. As shown in

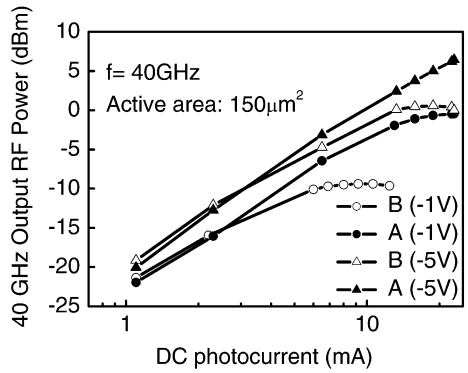

Fig. 5. RF power versus dc photocurrent of Device A and Device B under different reverse bias voltages (closed triangle: −5 V of Device A; open triangle: −5 V of Device B; closed circle: −1 V of Device A; open circle: −1 V of Device B) at 40-GHz operating frequency. The active area of both devices is 150 μm^2.

Fig. 4, the device with smallest geometry size has the largest RF power generation under the same photocurrent due to its smallest *RC* bandwidth limitation [15]. However, the maximum RF output power increases as the increase of active area of device. The observed phenomenon can be attributed to less density of photogenerated carriers and less space charge screening effect [15] of device with larger geometry size. In order to study the saturation behavior of devices clearly, we have measured several data points under high current operation (>10 mA). We can see that the −1-dB compression current and output RF power of device with 150-μm^2 active area are over 23 mA and 6.5 dBm, respectively. The shown maximum output powers and currents of different devices are limited by their failure. The obtained values of maximum power and current are much higher than the previous work on p-i-n ECPDs with integrated tapers [3], [4], [10] at the same operating frequency (40 GHz). To our knowledge, this is the highest saturation current bandwidth product and RF power (over 920 mA · GHz versus 6.5 dBm) reported with such a high responsivity (1.01 A/W). Fig. 5 shows the photogenerated RF power versus dc photocurrent of Devices A and B with the same active area (150 μm^2) under different reverse bias voltages (− and −5 V). As Fig. 5 indicates, both devices exhibit significant saturation behaviors under low bias voltage (−1 V) and high current operation (∼10 mA). Besides, Device A has significant higher values of RF saturation power then Device B especially under low dc bias voltage (−1 V). Under high dc bias voltage regime (−5 V), the obtained saturation current (∼13 mA) of Device B is close to that of the previous works on ECPD (∼11 mA) [10]. These measurement results, as shown in Figs. 2–5, indicate that the technique of partially p-doped photoabsorption layer will enhance the speed and output power performance of photodiode significantly without sacrificing the responsivity performance. The improvement in high-power performance of photodiode is due to the fact that the partially p-doped region can shorten the depletion width of the photoabsorption layer, reduce the space charge field of photogenerated carriers, and increase the output saturation current effectively [1]. Furthermore, as compared to downscaling the thickness of intrinsic InGaAs photoabsorption layer directly, this demonstrated technique would not increase the device absorption length or sacrifice the responsivity.

In conclusion, by utilizing the technique of partially p-doped photoabsorption layer, the demonstrated ECPD has significant improvement in high-power performance without sacrificing its speed and responsivity performance. State-of-the-art performance has been achieved simultaneously: very high responsivity (1.01 A/W), broad bandwidth (around 50 GHz), and over 6.5-dBm output RF saturation power with corresponding 920 mA · GHz current bandwidth product at 40-GHz operating frequency.

REFERENCES

[1] K. Kato, "Ultrawide-band/high-frequency photodetectors," *IEEE Trans. Microw. Theory Tech.*, vol. 47, no. 7, pp. 1265–1281, Jul. 1999.

[2] L. Y. Lin, M. C. Wu, T. Itoh, T. A. Vang, R. E. Muller, D. L. Sivco, and A. Y. Cho, "High-power high-speed photodetectors design, analysis, and experiment demonstration," *IEEE Trans. Microw. Theory Tech.*, vol. 45, no. 8, pp. 1320–1331, Aug. 1997.

[3] F. Xia, J. K. Thomson, M. R. Gokhale, P. V. Studenkov, J. Wei, W. Lin, and S. R. Forrest, "A asymmetric twin-waveguide high-bandwidth photodiode using a lateral taper coupler," *IEEE Photon. Technol. Lett.*, vol. 13, no. 8, pp. 845–847, Aug. 2001.

[4] S. Demiguel, L. Giraudet, L. Joulaud, J. Decobert, F. Blache, V. Coupe, F. Jorge, P. Pagnod-Rossiaux, E. Boucherez, M. Achouche, and F. Devaux, "Evanescently coupled photodiodes integrating a double-stage taper for 40-Gb/s applications-compared performance with side-illuminated photodiodes," *J. Lightw. Technol.*, vol. 20, no. 12, pp. 2004–2014, Dec. 2002.

[5] T. Takeuchi, T. Nakata, K. Makita, and T. Torikai, "A high-power and high-efficiency photodiodes with an evanescently coupled graded-index waveguide for 40-Gb/s applications," in *Proc. OFC 2001*, vol. 3, pp. WQ2-1–WQ2-3.

[6] H. Ito, S. Kodama, Y. Muramoto, T. Furuta, T. Nagatsuma, and T. Ishibashi, "High-speed and high-output InP–InGaAs unitraveling-carrier photodiodes," *IEEE J. Sel. Topics Quantum Electron.*, vol. 10, no. 4, pp. 709–727, Jul./Aug. 2004.

[7] X. Li, N. Li, S. Demiguel, X. Zheng, J. C. Campbell, H. H. Tan, and C. Jagadish, "A partially depleted absorber photodiode with graded doping injection regions," *IEEE Photon. Technol. Lett.*, vol. 16, no. 10, pp. 2326–2328, Oct. 2004.

[8] J.-W. Shi, K. G. Gan, Y.-H. Chen, C.-K. Sun, Y. J. Chiu, and J. E. Bowers, "Ultra-high power-bandwidth product and nonlinear photoconductance performances of low-temperature-grown GaAs based metal-semiconductor-metal traveling-wave photodetectors," *IEEE Photon. Technol. Lett.*, vol. 14, no. 11, pp. 1587–1589, Nov. 2002.

[9] Y. Muramoto and T. Ishibashi, "InP/InGaAs *pin* photodiode structure maximizing bandwidth and efficiency," *Electron. Lett.*, vol. 39, pp. 1749–1750, Nov. 2003.

[10] S. Demiguel, N. Li, X. Li, X. Zheng, J. Kim, J. C. Campbell, H. Lu, and A. Anselm, "Very high-responsivity evanescently coupled photodiodes integrating a short planar multimode waveguide for high-speed applications," *IEEE Photon. Technol. Lett.*, vol. 15, no. 12, pp. 1761–1763, Dec. 2003.

[11] J. Wei, F. Xia, and S. R. Forrest, "A high-responsivity high-bandwidth asymmetric twin-waveguide coupled InGaAs-InP-InAlAs avalanche photodiode," *IEEE Photon. Technol. Lett.*, vol. 14, no. 11, pp. 1590–1592, Nov. 2002.

[12] J.-W. Shi, Y.-S. Wu, F.-H. Huang, and Y.-J. Chan, "High-responsivity, high-speed, and high-saturation-power performances of evanescently coupled photodiodes with partially p-doped photo-absorption layer," in *IEDM Tech. Dig.*, Dec. 2004, pp. 351–354.

[13] S. Kawanishi and M. Saruwatari, "A very wide-band frequency response measurement system using optical heterodyne detection," *IEEE Trans. Instrum. Meas.*, vol. 38, no. 2, pp. 569–573, Apr. 1989.

[14] Z.-Y. Chen, Y.-L. Wang, Y. Liu, and N.-H. Zhu, "Two-port calibration of test fixtures with OSL method," in *Proc. 2002 3rd Int. Conf. Microwave and Millimeter Wave Technology*, pp. 138–141.

[15] A. Hirata, M. Harada, and T. Nagatsuma, "120-GHz wireless link using photonic techniques for generation, modulation, and emission of millimeter-wave signals," *J. Lightw. Technol.*, vol. 21, no. 10, pp. 2145–2153, Oct. 2003.